Electronic Supplementary Material (ESI) for Polymer Chemistry.

Supporting Information

Influence of Single Chain Nanoparticle Stabilizers on Polymerization Induced Hierarchical Self-Assembly

Wei Wen,[a] Aihua Chen*[,a,b]

[a] School of Materials Science and Engineering, Beihang University, Beijing 100191, P. R. China
[b] Beijing Advanced Innovation Centre for Biomedical Engineering, Beihang University, Beijing 100191, P. R. China

E-mail: chenaihua@buaa.edu.cn

Synthesis of $PDMAEMA_{51}$ macro-CTAs via RAFT solution polymerization

DMAEMA (8.00 g, 50.89 mmol), CPADB (0.24 g, 0.85 mmol), AIBN (0.028 g, 0.17 mmol) and 1,4-dioxane (10 mL) were added into a reaction tube and degassed by three freeze-pump-thaw cycles. The reaction tube was sealed under vacuum before placed in an oil bath at 70 °C. After 5 h, the reaction was quenched by liquid nitrogen. The reaction mixture was precipitated in petroleum ether for three times. The macro-CTAs were purified via dialysis (molecular weight cutoff of 3500 Da) in ethanol for two days. The degree of polymerization (DP) of the obtained macro-CTAs was measured by ^{1}H NMR (DP=51). The gel permeation chromatography (GPC) measurement (polystyrene standards) reveals an average number molecular weight (M_n) of 8.0 kg/mol and a polydispersity (M_w/M_n) of 1.11.

Characterizations

^{1}H NMR spectra were recorded on a Bruker DMX Spectrometer (400MHz), using $CDCl_3$ or $CDCl_3/d_6$-DMSO as solvent. For SCNP-CTAs, gel permeation chromatography (GPC) measurement was conducted on the system equipped with Agilent HPLC pump, Wyatt Technology detector and Agilent mixed columns (Plgel 20 μm MIXED-A and PLgel 10 μm MIXED-B), DMF with LiBr (0.05 mol/L) was used as the eluent with a flow rate of 1 mL/min at 25 °C. For linear BCPs, Waters 2410 GPC equipped with two columns (Styragel column: HR 4, 5 μm, 7.8 mm × 300 mm, 5-600 K; Styragel column: HR 2, 5 μm, 7.8 mm × 300 mm, 500-20K) was used to analyze the molecular weight and dispersion and THF was used as the eluent with a flow rate of 1 mL/min at 25 °C. For BCPs with intrachain cross-linked stabilizer, GPC were not conducted because of their poor solubility in common solvents, such as DMF, THF and methanol. The transmission electron microscopy (TEM) observation was carried out on a JEM-2100 microscope with an accelerating voltage of 200 kV. For sample preparation, one drop of the diluted micellar solution was cast on a carbon-coated copper grid and dried at room temperature. The samples were stained by RuO_4 for two minutes. The scanning electron microscopy (SEM) observation was performed on a TESCON MAIA3 microscope with an accelerating voltage of 5 kV. For sample preparation, one

drop of the diluted micellar solution was cast on a cleansed silicon wafer and dried at room temperature. The samples were treated by spray-gold. The atomic force microscopy (AFM) height images were collected with a Bruker Resolve probe microscope under tapping mode. One drop of dilute micellar solution was deposited on a cleansed silicon wafer. The solvent was evaporated at room temperature before measurement. Dynamic light scattering (DLS) were analyzed using a Malvern Zetasizer Nano ZS90 instrument. DLS provides the hydrodynamic (*z*-average) diameter and polydispersity index (PDI). Differential scanning calorimetry (DSC) analyses were performed by NETZSCH DSC214 instrument. The DSC samples were scanned under air flow from 25 ^{o}C to 200 ^{o}C at a heating/cooling rate of ±10 ^{o}C /min. The data of the first cooling processes and second heating processes were recorded. Small-angle X-ray scattering (SAXS) of the as-prepared assemblies was measured at Shanghai Synchrotron Radiation Facility (SSRF, BL16B1 beamline) with an X-ray wavelength of 1.24 Å and the distance from sample to detector is 1947.5 mm. Polarized optical microscopic (POM) experiments were done using Shang Guang 59XF microscope. A drop of micellar solution was dropped to the glass slide without any treament before observation.

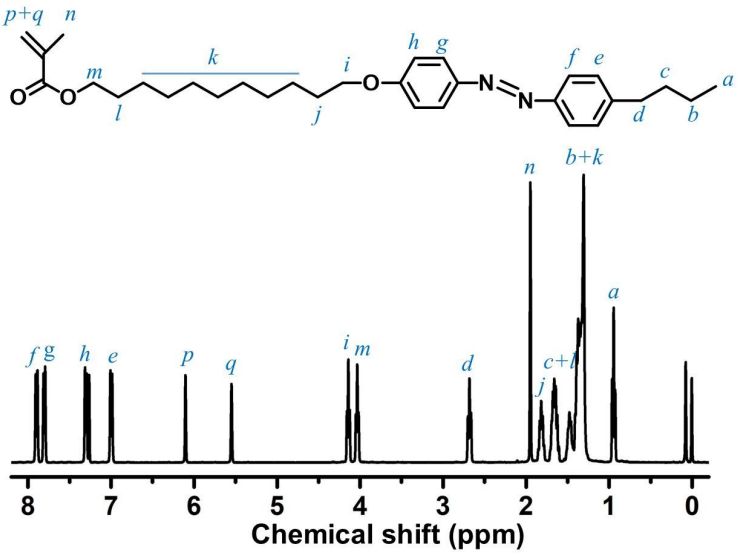

Fig. S1 Chemical structure and ^{1}H NMR spectrum of MAAz monomer.

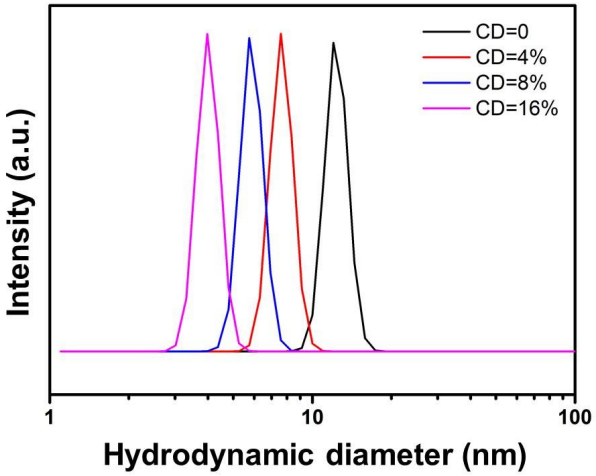

Fig. S2 Hydrodynamic diameter of linear PDMAEMA$_{51}$-CTA (black line) and the resultant PDMAEMA(SCNP)$_{51}$-CTA with varied CDs through intrachain cross-linking, measured by DLS.

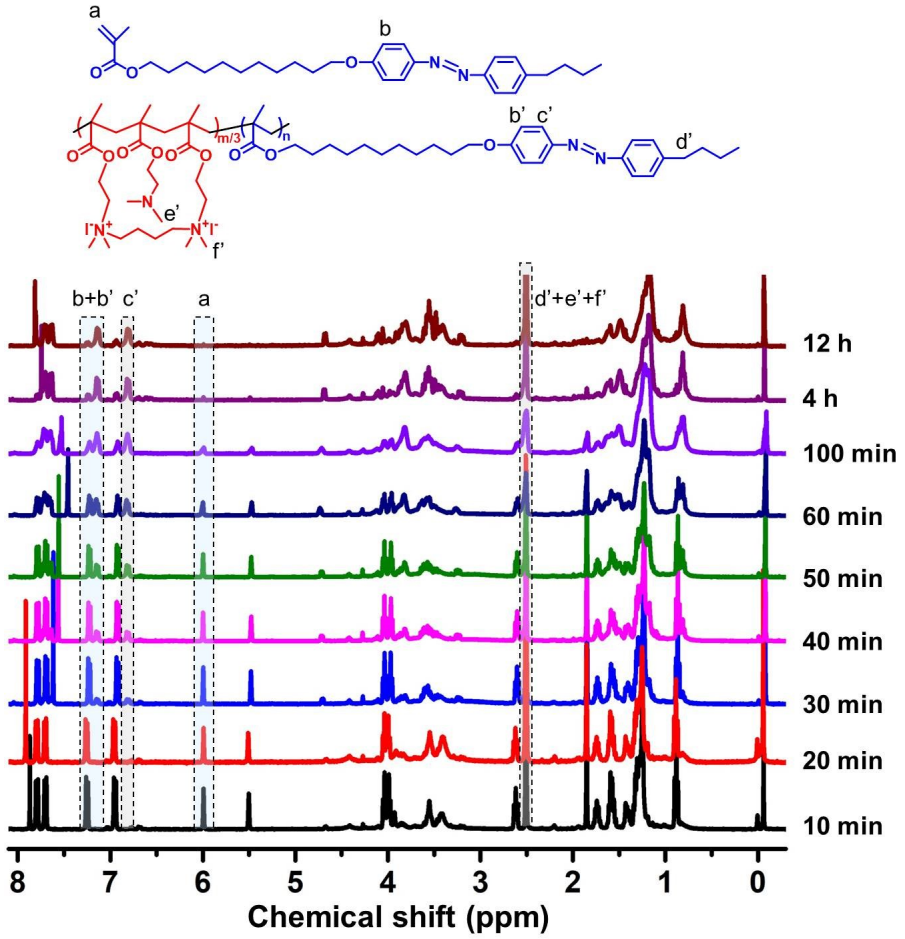

Fig. S3 ^{1}H NMR spectra of target PDMAEMA(SCNP)$_{51}$-*b*-PMAAz$_{100}$ at different polymerization times, using $CDCl_3$/d_6-DMSO as solvent. Conditions: CD of PEMAEMA(SCNP)$_{51}$-CTA is fixed at 8%; [PDMAEMA(SCNP)-CTA]/[MAAz]/[AIBN] molar ratio= 1:100:0.2; total solid content = 15% w/w. MAAz monomer conversion was calculated based on the peaks at 5.98 (*a*) and 7.08-7.26 (*b+b'*) ppm. M_n was calculated based on the peaks at 6.80 (*c'*) and 2.47-2.52 (*d'+e'+f'*) ppm.

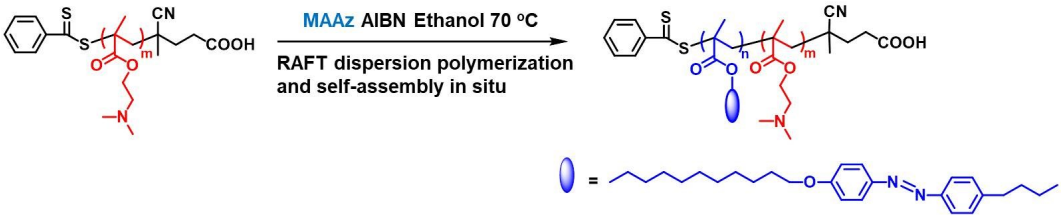

Scheme S1 Synthetic route to linear PDMAEMA$_{51}$-*b*-PMAAz$_n$ NPs via RAFT dispersion polymerization in ethanol.

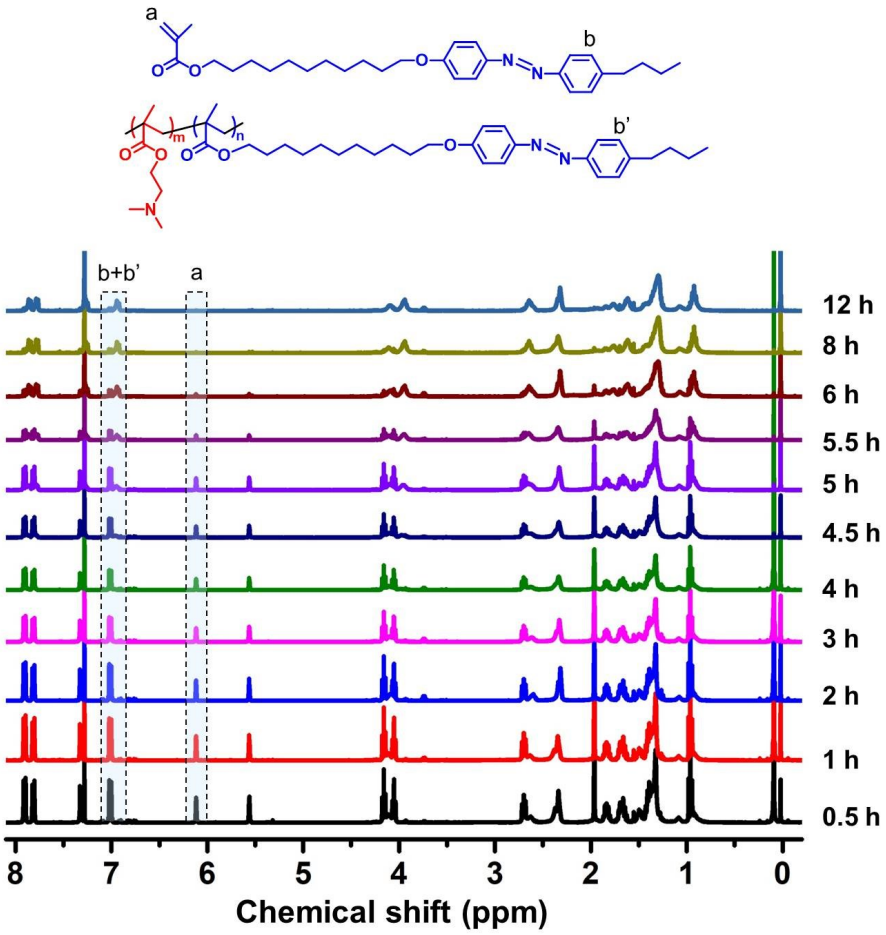

Fig. S4 ^{1}H NMR spectra of target linear PDMAEMA$_{51}$-*b*-PMAAz$_{100}$ at different polymerization times, using $CDCl_3$ as solvent. Conditions: [PDMAEMA-CTA]/[MAAz]/[AIBN] molar ratio = 1:100:0.2; total solid content = 15% w/w. MAAz monomer conversion was calculated based on the peaks at 6.11 (*a*) and 6.91-7.03 (*b+b'*) ppm.

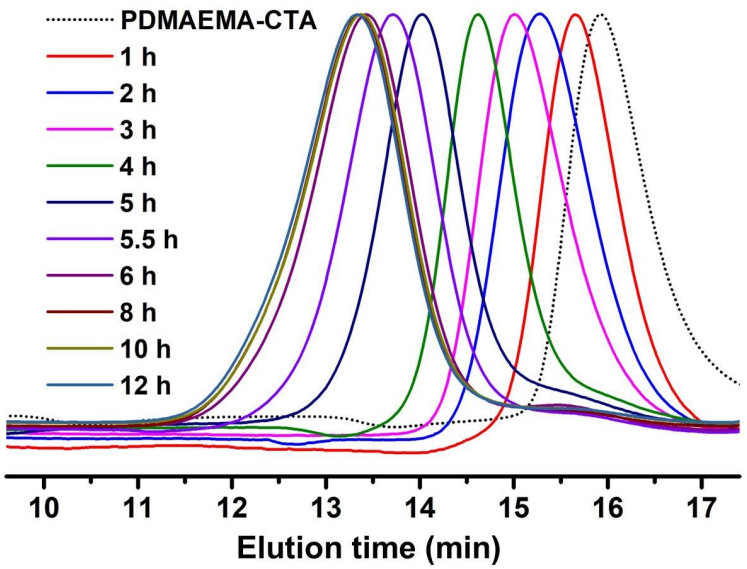

Fig. S5 GPC curves of linear PDMAEMA$_{51}$-CTAs and target PDMAEMA$_{51}$-*b*-PMAAz$_{100}$ at different polymerization times, THF was used as the eluent. Conditions: [PDMAEMA-CTA]/[MAAz]/[AIBN] molar ratio= 1:100:0.2; total solid content = 15% w/w.

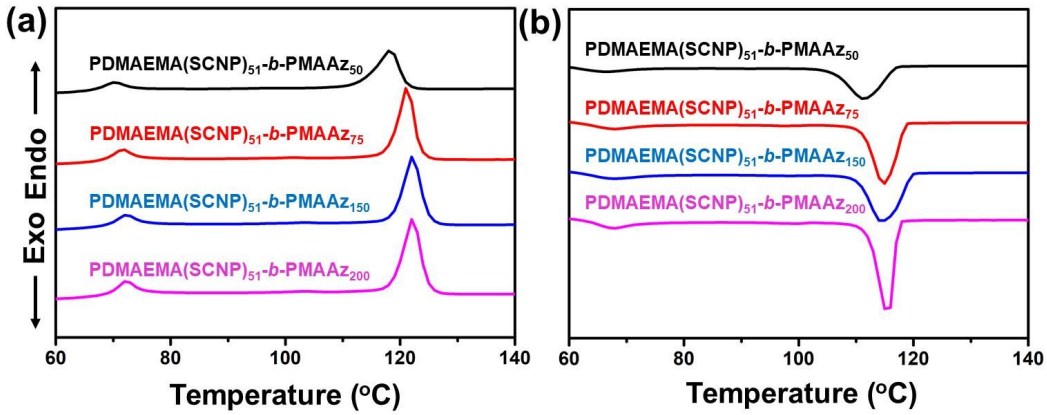

Fig. S6 DSC curves for PDMAEMA(SCNP)$_{51}$-*b*-PMAAz$_n$ NPs during the (a) second heating and (b) first cooling processes.

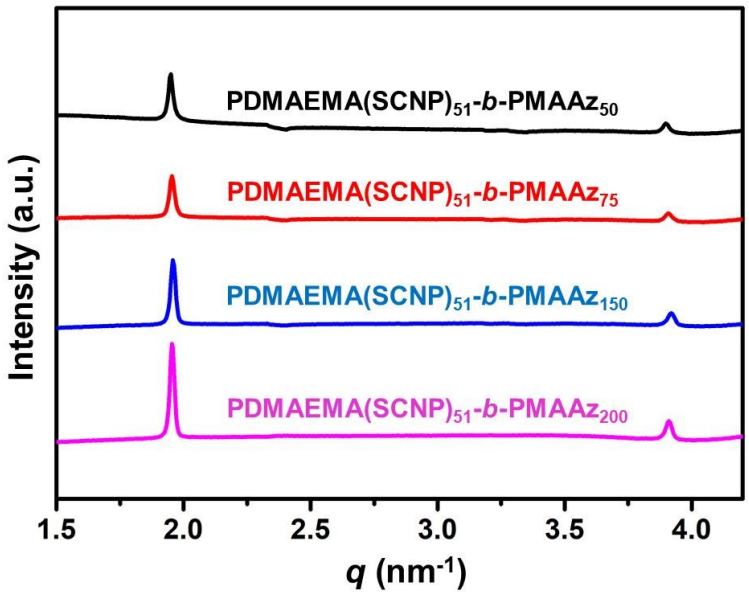

Fig. S7 SAXS patterns of PDMAEMA(SCNP)$_{51}$-*b*-PMAAz$_n$ NPs dispersion in ethanol.

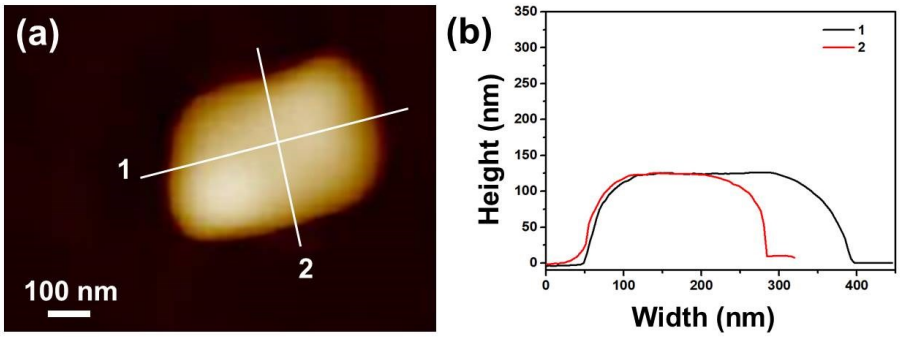

Fig. S8 (a) AFM image and (b) the corresponding height profiles of PDMAEMA(SCNP)$_{51}$-*b*-PMAAz$_{75}$ NPs via PIHSA. Conditions: CD of PEMAEMA(SCNP)-CTA is 8%; total solid content = 15% w/w.

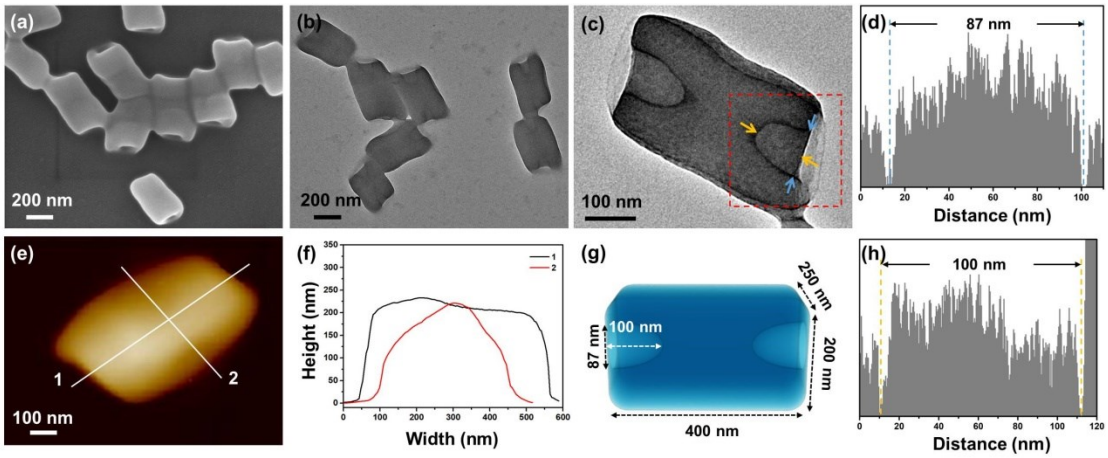

Fig. S9 (a) SEM image, (b) TEM image, unstained, (c) magnified TEM image, stained by RuO_4, (e) AFM image and (f) the corresponding height profiles of holbrick-like NPs prepared from PDMAEMA(SCNP)$_{51}$-*b*-PMAAz$_{100}$ via PISA. The intensity profiles of the (d) width and (h) depth of the hollow are measured by TEM across the hollow, corresponding to the blue and yellow arrows in (c). (g) A model of the holbrick-like NPs. Conditions: CD of PEMAEMA(SCNP)$_{51}$-CTA is 8%; total solids concentration = 15% w/w.

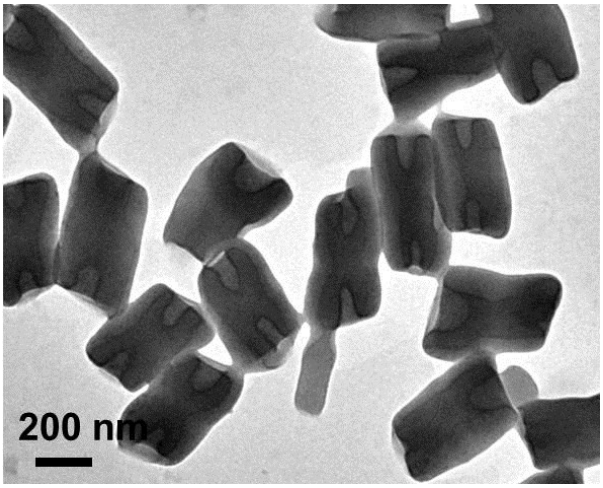

Fig. S10 TEM image of holbrick-like NPs after 24 months.

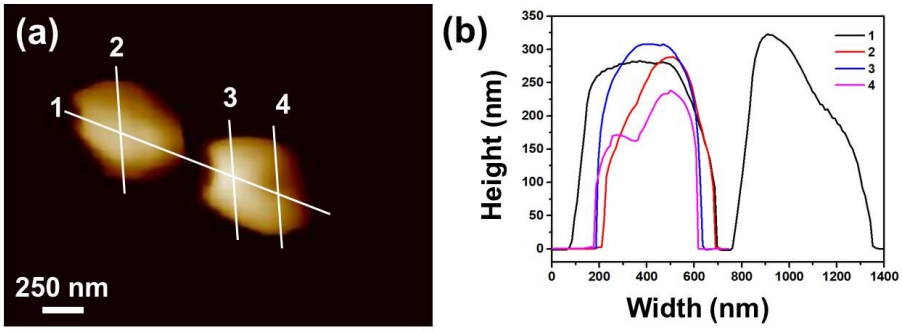

Fig. S11 (a) AFM image and (b) the corresponding height profiles of PDMAEMA(SCNP)$_{51}$-*b*-PMAAz$_{150}$ NPs via PIHSA. Conditions: CD of PEMAEMA(SCNP)$_{51}$-CTA is fixed at 8%; total solid content = 15% w/w.

Table S1. Characterization data for PDMAEMA(SCNP)$_{51}$-*b*-PMAAz$_n$ NPs with different DP$_{PMAAz}$ and CD of PDMAEMA(SCNP)$_{51}$.

Sample[a]	M_n (kg/mol)[b]	Cross-linking degree of SCNP (%)	Hydrodynamic diameter (nm)	PDI[c]	Morphology[d]
PDMAEMA(SCNP)$_{51}$-*b*-PMAAz$_{20}$	16.8	8	105	0.103	spherical NPs
PDMAEMA(SCNP)$_{51}$-*b*-PMAAz$_{35}$	23.4	8	133	0.146	spherical/cuboidal NPs
PDMAEMA(SCNP)$_{51}$-*b*-PMAAz$_{50}$	30.9	8	148	0.249	cuboidal NPs
PDMAEMA(SCNP)$_{51}$-*b*-PMAAz$_{75}$	42.3	8	209	0.158	cuboidal NPs
PDMAEMA(SCNP)$_{51}$-*b*-PMAAz$_{100}$	53.8	8	297	0.198	holbrick-like NPs
PDMAEMA(SCNP)$_{51}$-*b*-PMAAz$_{150}$	76.6	8	391	0.015	jujube-like NPs
PDMAEMA(SCNP)$_{51}$-*b*-PMAAz$_{200}$	99.5	8	452	0.121	jujube-like NPs
PDMAEMA(SCNP)$_{51}$-*b*-PMAAz$_{100}$	55.7	2	174	0.105	cuboidal NPs
PDMAEMA(SCNP)$_{51}$-*b*-PMAAz$_{100}$	54.7	4	197	0.066	cuboidal NPs
PDMAEMA(SCNP)$_{51}$-*b*-PMAAz$_{100}$	52.8	16	432	0.041	jujube-like NPs
PDMAEMA(SCNP)$_{51}$-*b*-PMAAz$_{100}$	51.3	32	493	0.180	jujube-like NPs

[a]The DPs of PMAAz are targeting values.

[b]The M_n were determined by ^{1}H NMR spectra.

[c]Polydispersity (PDI) measured by DLS.

[d]The morphology identified by TEM.

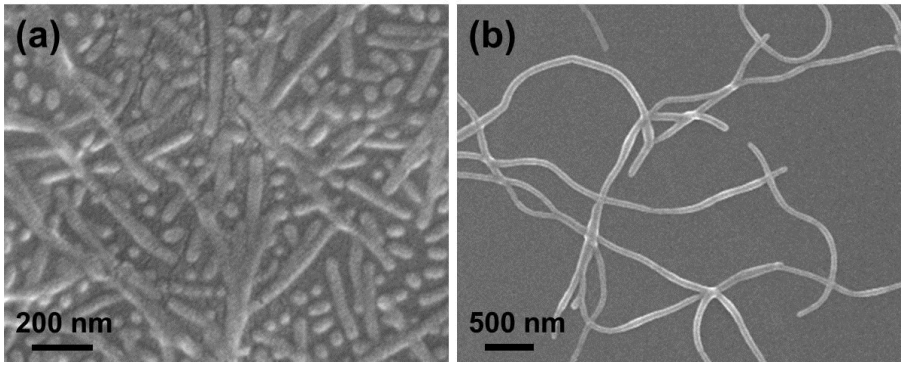

Fig. S12 SEM images of linear (a) PDMAEMA$_{51}$-*b*-PMAAz$_{50}$, and (b) PDMAEMA$_{51}$-*b*-PMAAz$_{100}$ NPs. Total solid content = 15% w/w.

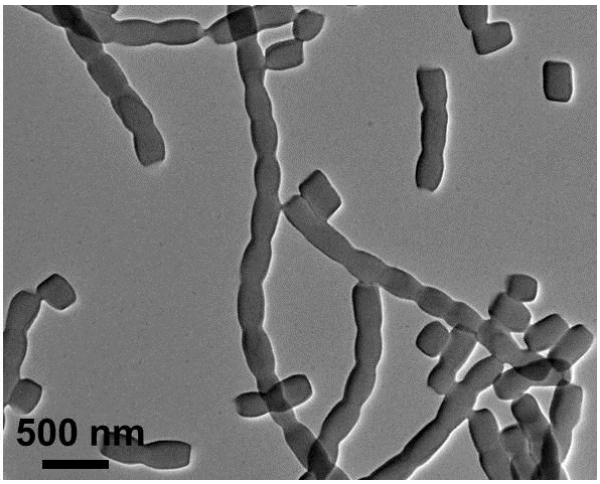

Fig. S13 TEM images of charged PDMAEMA(iodoethane)$_{51}$-*b*-PMAAz$_{100}$ NPs. Total solid content = 15% w/w. The preparation of PDMAEMA(iodoethane)$_{51}$-CTAs was similar to PDMAEMA(SCNP)$_{51}$-CTAs. The zeta potential value of the necklace-like nanowires in ethanol is + 21.8 mv, similar to that of the PDMAEMA(SCNP)$_{51}$-*b*-PMAAz$_{100}$ NPs (+ 21.3 mv).

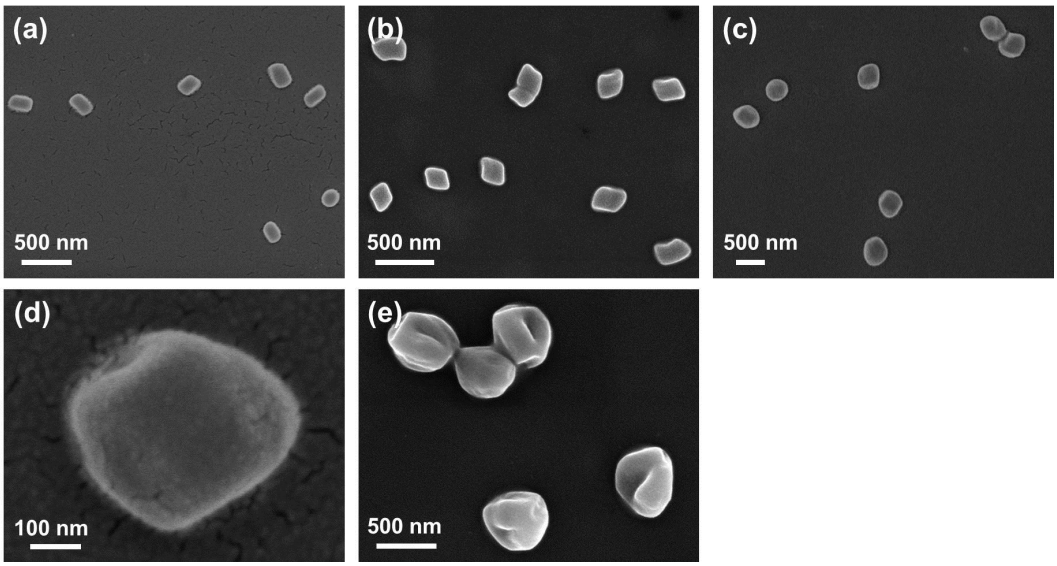

Fig. S14 SEM images and magnified SEM images of PDMAEMA(SCNP)$_{51}$-*b*-PMAAz$_{100}$ NPs with different CDs of PDMAEMA(SCNP)$_{51}$: (a) 2%, (b) 4%, (c-d) 16%, and (e) 32%. Total solid content = 15% w/w.

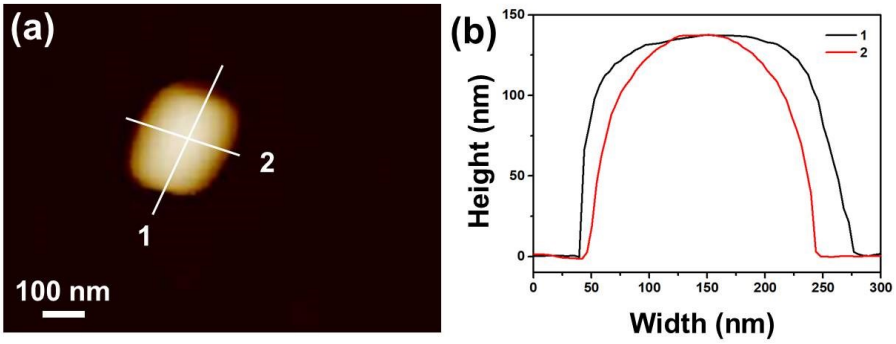

Fig. S15 (a) AFM image and (b) the corresponding height profiles of PDMAEMA(SCNP)$_{51}$-*b*-PMAAz$_{100}$ NPs with 5% w/w solid content. CD of PEMAEMA(SCNP)-CTA is 8%.